RF TUNING OF THE KEK 40 MeV PROTON LINAC WITH POST COUPLERS

T. Kato and S. Machida
National Laboratory for High Energy Physics
Oho-machi, Tsukuba-gun, Ibaraki-ken, 305, Japan

Summary

An Alvarez linac was constructed to increase the output energy from 20 MeV to 40 MeV at KEK. The new tank was stabilized by post couplers and the flatness of the TM010 field distribution was within ± 0.7 %. Equivalent circuit analysis which numerically solves the loop equations including stem and post currents in addition to tank current corresponding to the accelerating field explains rf characteristics of a post-coupled structure.

Introduction

Instead of proton multiturn injection into the Booster Synchrotron, H^- charge-exchange injection was adopted at KEK since June 1985. For the higher intensity of the beam in the Booster, extension of the linac was planned to increase its output energy from 20 MeV to 40 MeV. In 1983, a model tank was built for studying rf characteristics of the post-stabilized tank[1]. Then a new tank was designed and constructed[2]. There are two features in the tank; one is the application of permanent quadrupole magnets for transverse focusing[2], and the other is the utilization of post couplers for stabilization of the tank. In this paper, the tuning of the tank by post couplers including the analysis with an equivalent circuit is described.

Structure of the tank

The new tank of 0.9 m in diameter and 12.844 m in length consists of four sub-tanks and contains 34 full drift tubes and 2 half drift tubes at the ends. Diameters of the drift tubes and the stems are 160 mm and 36 mm. The ratio of gap to cell length changes from 0.2456 to 0.3187. 12 frequency tuners of 125 mm in diameter are prepared to shift the resonant frequency and change the axial field locally. They can change the resonant frequency about 340 kHz. Furthermore two frequency tuners of 115 mm in diameter are prepared to tune the resonant frequency automatically to that of the 20 MeV old tank with a feedback circuit. 34 post couplers of 30 mm in diameter are installed alternately from both sides of the tank toward the center of the drift tube. Elliptical tabs of 66 mm in the major axis, 38 mm in the minor axis and 20 mm in thickness are attached to the inner end of post couplers. They turn 180 degrees and move in and out about 160 mm. Two rf loop couplers located at 1/4 and 3/4 of the tank are used to deliver an rf power.

Equivalent circuit analysis

An equivalent circuit used[3] is shown in Fig. 1. Notation in Fig. 1 follows reference (4). There are six unknowns, a tank current corresponding to the accelerating field I(n,1), three stem currents I(n,2), I(n,3) and I(n,4) and two post currents I(n,5) and I(n,6) for the n-th circuit. Total number of unknowns for a N-coupled chain is 6(N-1) + 1. Therefore, (6N-5) equations are numerically solved to obtain three kinds of currents, that is, Itank(n) = I(n,1), Istem(n) = I(n,2) + I(n,3) + I(n,4) and Ipost(n) = I(n,5) + I(n,6). Using Kirchhoff's law, the loop equations for the n-th circuit are written as follows.

$$V_{c,n}=I(n,2)/2j\omega C_1 \quad (1)$$
$$V_{c,n}-V_n=j\omega L_0(1-\omega_0^2/\omega^2)I(n,1)+j\omega M_0 I(n+1,1) \quad (2)$$
$$V_{n+1}-V_{c,n}=j\omega L_0(1-\omega_0^2/\omega^2)I(n+1,1)+j\omega M_0 I(n,1) \quad (3)$$
$$V_{c,n}=j\omega L_1 I(n,3)+j\omega M_1 I(n-1,4) \quad (4)$$
$$V_{c,n}=j\omega L_1 I(n,4)+j\omega M_1 I(n+1,3) \quad (5)$$
$$V_{c,n}=j\omega L_2 I(n,5)+I(n,5)/j\omega C_2+j\omega M_2 I(n-1,6) \quad (6)$$
$$V_{c,n}=j\omega L_2 I(n,6)+I(n,6)/j\omega C_2+j\omega M_2 I(n+1,5) \quad (7)$$
$$I(n+1,1)=\sum_{m=1,6} I(n,m) \quad (8)$$

where $\omega_0^2 = 1/L_0C_0$ and ω is a driving frequency. If equations from (2) to (7) are rearranged using equation (1), and if equation (3) for the (n-1)-th circuit and equation (2) for the n-th circuit are added together, it becomes the following equations for the n-th circuit,

$$2(1-\omega_0^2/\omega^2)I(n,1)+(\omega_1^2/2\omega^2)I(n,2) -(\omega_1^2/2\omega^2)I(n-1,2)+k_0 I(n-1,1)+k_0 I(n+1,1)=0 \quad (9)$$
$$(\omega_3^2/2\omega^2)I(n,2)+I(n,3)+k_1 I(n-1,4)=0 \quad (10)$$
$$(\omega_3^2/2\omega^2)I(n,2)+I(n,4)+k_1 I(n+1,3)=0 \quad (11)$$
$$I(n,3)-k_4(1-\omega_2^2/\omega^2)I(n,5)+k_1 I(n-1,4)-k_2 I(n-1,6)=0 \quad (12)$$
$$I(n,4)-k_4(1-\omega_2^2/\omega^2)I(n,6)+k_1 I(n+1,3)-k_2 I(n+1,5)=0 \quad (13)$$
$$I(n+1,1)=\sum_{m=1,6} I(n,m) \quad (14)$$

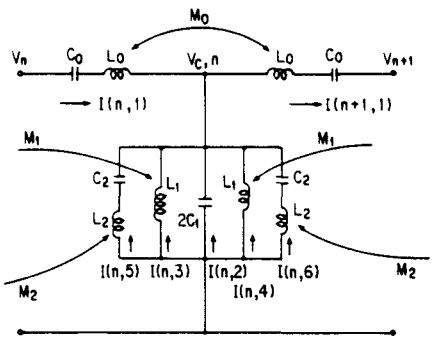

Fig. 1 Equivalent circuit of a post-coupled structure.

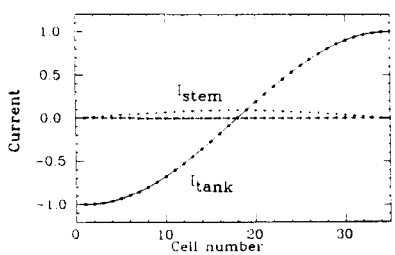

Fig. 2 Calculated mode of a 35 cell tank without post couplers (TM011 like). Free parameters are given as follows. ω_0 = 210.8 MHz, ω_1 = 215.8 MHz, ω_3 = 93 MHz, k_0 = 0.1, k_1 = 0.095, k_4 = 0.71, ω = 201.31 MHz.

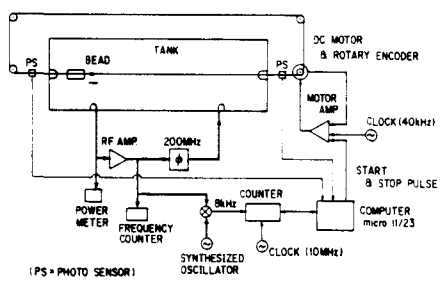

Fig. 3 Block diagram of the field measurement.

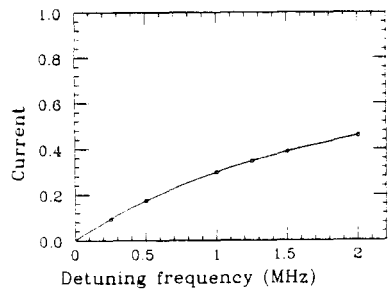

Fig. 4 Calculated sum of post currents at the stabilization when perturbation is given to the both end cells.

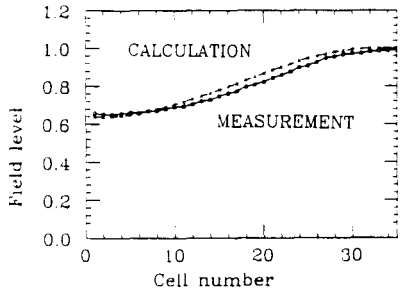

Fig. 5 Measured TM010 field when the post couplers were pulled out.

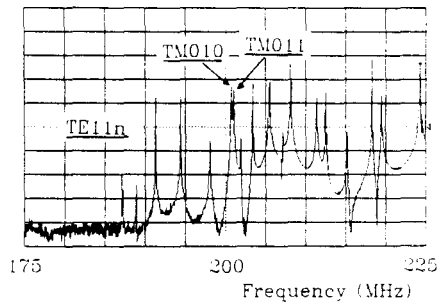

Fig. 6 Measured resonant modes of the post-less tank.

where $k_0 = M_0/L_0$, $k_1 = M_1/L_1$, $k_2 = M_2/L_1$, $k_4 = L_2/L_1$, $\omega_1^2 = 1/L_0C_1$, $\omega_2^2 = 1/L_2C_2$ and $\omega_3^2 = 1/L_1C_1$. Calculated currents are so normalized that the largest one among three kinds of currents in the tank is assumed to be 1. Figure 2 shows an example of the calculated mode.

Measurement method

The axial field was measured by usual bead perturbation technique as shown in Fig. 3. Some cares were taken to increase the accuracy. Phase-locked loop was used for stabilizing the speed of the bead. Its fluctuation was reduced to less than 0.01 %. Resonant frequency of the self-excited circuit including the tank was stabilized with suitable gain and phase of the feedback amplifiers. Reference frequency producing the beat frequency of 8 kHz was delivered from a synthesized oscillator. Two photo-sensors were used to detect the passing of the bead. They determined the location of the bead in the tank with the aid of 10 MHz clock. The accuracy of the measurement of the field averaged over a unit cell was less than 0.2 %.

We used another method of the field measurement, which is simple and useful when we want to identify the mode. If an external driving frequency is fixed on a shoulder of a resonant curve, for example, - 3dB down from center of the curve, a shift of the resonant frequency by the bead purturbation causes a change of the amplitude of the measured rf signal. Synthesized network analyser with a fixed driving frequency measures the signal mentioned above with high accuracy.

Tuning procedures

There are two important problems in the tuning of the tank; one is the stabilization of the tank using post couplers, and the other is the tuning of the resonant frequency to 201.07 MHz, which is the value of the old tank. The latter is important since the field distribution tuned by frequency tuners affects the amount of excitation of the post modes when stabilization is achieved as shown in Fig. 4.

As the design of the field distribution over the tank is uniform, the stabilization of the tank means that the distortion parameter D_x is reduced to the minimum with post tuning,

$$D_x = \sum_{i=1,N} |E_i - E_{ave}|/N \qquad (15)$$

where E_i represents the field of the i-th cell, E_{ave} is the field averaged in the tank and N is total number of cells.

Accelerating field without post couplers

Figure 5 shows the measured field of TM010 mode when post couplers were pulled out exceedingly, that is, 155 mm away from the drift tubes. The field distribution over the tank inclines due to the effect of stems and post couplers and $D_x = 0.14$. In the design of the tank, the average effects of stems and post couplers on the resonant frequency were taken into acount. The result of calculation using the equivalent circuit is also shown. The frequency perturbation by stems and post couplers is given in such a way that the deviation from the resonant frequency of a unit cell varies at the uniform rate from 110 kHz to - 110 kHz in the tank.

Secondly, 14 frequency tuners were carefully inserted to make a nearly uniform field distribution and D_x became 0.0114. Then a 10 % tilt was given to the field distribution by the frequency tuners of No.1 and No.14. D_x was 0.0306. The above procedure was useful to find the stabilizing point clearly. The measured resonant modes are shown in Fig. 6.

Tuning with post couplers

When the post couplers were gradually inserted into the tank, TE11n modes were strongly perturbed and finally a number of post modes appeared. As the post length, which means the distance between post coupler and drift tube, decreased, the frequencies of the post modes decreased. When the post band edge crossed TM010 mode, the field was strongly perturbed. Stabilization was achieved at the post length of 74 mm (Fig. 7) and the field distribution became flat as shown in

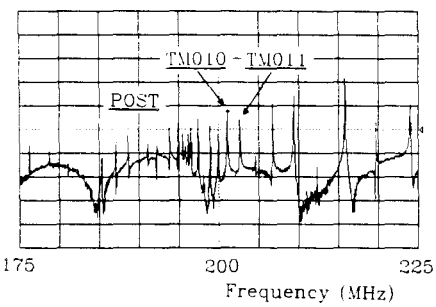

Fig. 7 Measured resonant modes at the stabilization.

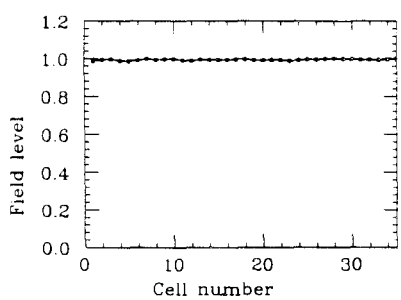

Fig. 8 Measured TM010 field at the stabilization.

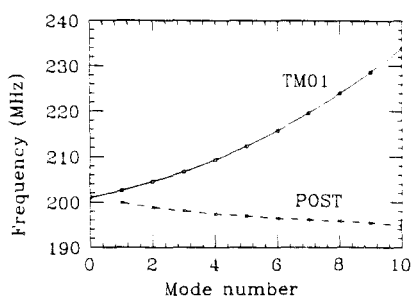

Fig. 9 Measured dispersion relation at the stabilization.

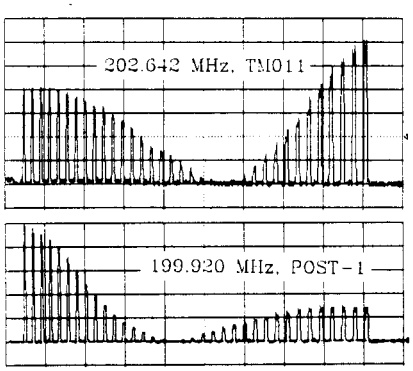

Fig. 10 Measured field variation on the axis at the stabilization. Upper is TM011. Lower is post-1 mode.

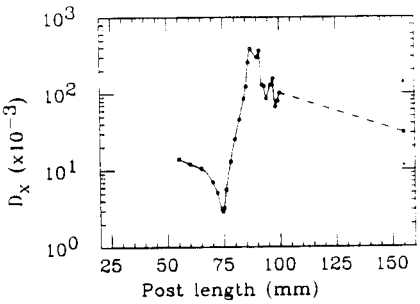

Fig. 11 Measured distortion parameter vs. post length.

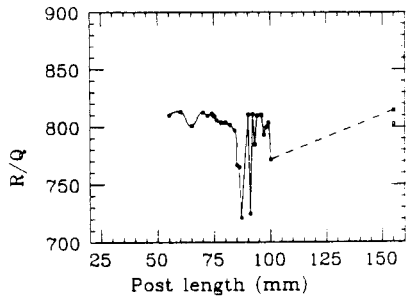

Fig. 12 Measured R/Q (MΩ/m) vs. post length.

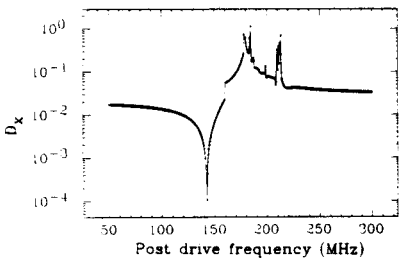

Fig. 13 Calculated distortion parameter vs. post frequency (ω_2). ω = 201.00 MHz, k_2 = - 0.09.

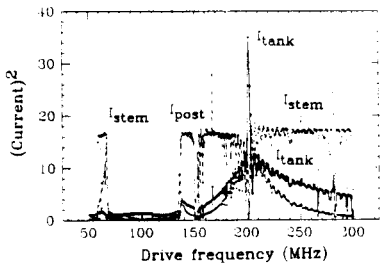

Fig. 14 Calculated modes at the stabilization. ω_2 = 142.4 MHz.

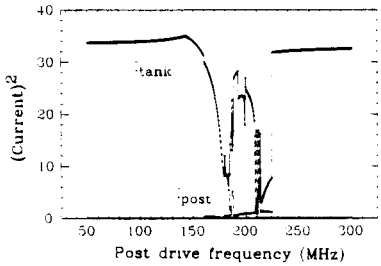

Fig. 15 Calculated sums of square of currents vs. post frequency (ω_2).

Fig. 8. With the aid of small tab rotation (within 25 degrees) of five post couplers, distortion parameter of 0.0029 was achieved and the field variation within ± 0.7 % was obtained. Dispersion relation at the stabilization is shown in Fig. 9. The mode separation between TM010 and TM011 increased from 0.3 MHz to 1.57 MHz at the stabilization. In addition to the stem modes ranging from 73 MHz to 81 MHz, 34 resonant modes were observed below TM010 mode probably corresponding to the post modes.

Figure 10 shows measured rf amplitude for TM011 and Post-1 modes with the bead perturbation on axis. Figure 11 shows variation of the distortion parameter during tuning. Variation of R/Q is shown in Fig. 12.

Simulation using equivalent circuit

The equivalent circuit well explains the behavior of the distortion parameter during post tuning as shown in Fig. 13. The calculated three kinds of sums of square of currents for all cells at the stabilization are represented in Fig. 14. The calculated sums of square of currents for all cells versus post frequency ω_2 are shown in Fig. 15.

Resonant frequency of TM010 mode

The model tank study predicted the deviation of the resonant frequency from SUEPRFISH calculation as follows,

increase by post couplers	114 kHz,
increase by stems	330 kHz,
variation by tuners	± 179 kHz,
decrease by errors	- 253.5 kHz,

In the above, the decrease by errors is mainly due to the mesh size in the SUPERFISH calculation. Then the calculated frequency of 200.63 MHz was chosen since the goal was 201.07 MHz and safety factor of - 70 kHz was taken into account.

The deviation of the resonant frequencies from the estimation became - 2 kHz for the post-less tank and - 10 kHz for the stabilized tank provided that the changes of the frequency due to the temperature and the atmosphere are - 2.9 kHz/degree and 62 kHz.

Q values and transit time factor

Q value varied during post tuning as follows,

post-less tank	64900,
decrease by 12 tuners	- 2500,
decrease by auto-tuners	- 1400,
decrease by post couplers	- 3900,
stabilized tank	57100,
calculation without stems	79100.

Shunt impedance of the stabilized tank is 46 MΩ/m.

Measured transit time factors vary from 0.878 to 0.821, which are larger than calculated values by 0.69 % on the average.

Acknowledgment

The authors wish to express their gratitude to Prof. S. Fukumoto for valuable discussion and encouragement. They thank Dr. E. Takasaki, members of the injector group and Mr. Y. Iino and his group of Mitsubishi Heavy Industries for their help during measurement.

References

1. S. Machida et al., IEEE Trans. Nucl. Sci. NS-32, 3259 (1985).
2. S. Fukumoto et al., Proc. 1984 Linear Accelerator Conf., 135, 1984.
3. T. Nishikawa, 'A note on the dispersion relation of the Los Alamos structure for the drift tube linac', 1967, unpublished.
4. G. Dôme, Linear Accelerators edited by P.M. Lapostolle and A.L. Septier, Amsterdam, 1970, C.1.le, p.706.